Unthresholded Recurrence Plots for Complex-Valued Representations of Narrow Band Signals

Aloys Sipers, Paul Borm and Ralf Peeters

Abstract We address the information content of unthresholded recurrence plots for complex-valued signals admitting a Fourier series representation (including periodic and sampled signals). Unthresholded recurrence plots of complex-valued signals contain the information of two real-valued signals simultaneously and can therefore be used to study the relationship between these signals. The graph theoretic procedure in our recent work [1], which was developed to characterize the uniqueness conditions for real-valued signals, is extended to the class of complex-valued signals. The special properties of complex signal representations provide alternative ways to employ unthresholded recurrence plots on narrow band signals. Examples and an application from EEG analysis clarify the results.

1 Introduction

Recurrence plots (RPs) are a signal analysis method that was initially introduced to visualize characteristics of a trajectory in a phase space [2]. Later, to go beyond the visual impression, different measures of quantification of RPs were introduced, see [3, 4]. These techniques have been applied in a variety of different disciplines, such as finance, economy, earth sciences, biology, neuroscience, physiology, engineering, physics and chemistry. In the last decade an impressive increase of the application

A. Sipers (✉) · P. Borm
Centre of Expertise in Life Sciences, Zuyd University,
Nieuw Eyckholt 300, 6419 DJ Heerlen, The Netherlands
e-mail: aloys.sipers@zuyd.nl

P. Borm
e-mail: paul.borm@zuyd.nl

R. Peeters
Department of Knowledge Engineering, Universiteit Maastricht,
Bouillonstraat 8-10, 6200 MD Maastricht, The Netherlands
e-mail: ralf.peeters@maastrichtuniversity.nl

N. Marwan et al. (eds.), *Translational Recurrences*, Springer Proceedings
in Mathematics & Statistics 103, DOI 10.1007/978-3-319-09531-8_3

of methods based on RPs can be observed, see the bibliography collected on the website [5]. Some of the pitfalls which can occur during the application of RPs are highlighted in [6].

Given a finite-interval continuous-time real-valued signal $x(t)$, with $t \in [0, 1)$ say, its corresponding recurrence plot is constructed with the time-delay embedding method (cf. [7]) in three steps:

(1) An embedding dimension M and a time-delay $\tau \in (0, 1)$ are chosen, and an associated M-dimensional vector trajectory $X(t)$ is constructed as:

$$X(t) = \begin{pmatrix} x(t) \\ x(t+\tau) \\ \vdots \\ x(t+(M-1)\tau) \end{pmatrix}, t \in [0, 1). \tag{1}$$

Here, for technical convenience (to avoid having to take finite interval effects explicitly into account), the signal $x(t)$ is *periodically extended* from the interval $[0, 1)$ to all of $\mathbb{R}$.

(2) The *unthresholded* recurrence plot (URP) is defined as (the graph of) the intra-trajectory distance function $\mathrm{URP}_X(u, v)$, given by

$$\mathrm{URP}_X(u, v) = \|X(u) - X(v)\|, \quad u, v \in [0, 1), \tag{2}$$

in which $\|\cdot\|$ denotes the Euclidean norm.

(3) For a given positive threshold ε, the *binary* (thresholded) recurrence plot is defined as

$$\mathrm{RP}_X^{\varepsilon}(u, v) = \begin{cases} 1 & \text{if } \mathrm{URP}_X(u, v) \leq \varepsilon, \\ 0 & \text{if } \mathrm{URP}_X(u, v) > \varepsilon. \end{cases} \tag{3}$$

In this paper we study the information content of URPs of complex-valued signals. They are defined in a similar manner, with the Euclidean norm $\|\cdot\|$ in step (2) generalized to trajectories that are now in $\mathbb{C}^M$. This theoretical study on URPs of complex-valued signals is new and may serve as a starting point for applications of URPs and RPs on complex-valued signals which are constructed from real world data. Furthermore, the special properties of *complex signal representation* are used to employ URPs in alternative ways on signals with a narrow band power spectrum. The information content of URPs and RPs of real-valued signals has been studied in [1, 8–13], respectively.

In Sect. 2, we study the information content of URPs of zero mean continuous-time complex-valued signals on $[0, 1)$ which admit a Fourier series representation. We build upon our recent work of [1] where real-valued signals were analyzed. As in that case, we show that for any complex-valued signal its power spectrum is entirely determined by its URP, regardless of the choice of M and τ. It is easily seen that a URP does not carry information on the mean of a signal (hence the zero mean assumption), nor on a unimodular scaling factor, nor on complex conjugation. We provide sufficient

conditions on M and τ which guarantee that a zero mean complex-valued signal $w(t)$ can be *uniquely* recovered from its URP, up to conjugacy and a unimodular factor. They extend the necessary and sufficient conditions for real-valued signals given in [1]. In general, when these conditions are not satisfied, it depends on M, τ, and the frequency content of the actual signal $w(t)$ itself, which information can be recovered from its URP. These results have implications for real-valued signals too, because recurrence plots of complex-valued signals relate to *joint recurrence plots* for two real-valued signals; see [14].

In Sect. 3, we address another application of complex-valued signal representations by studying signals with a narrow band power spectrum. Then, in Sect. 4, the information content and the structure of URPs for narrow band signals are illustrated by two examples. First, we investigate four different settings for M and τ, which cause complex signals with magnitudes having different morphology to exhibit identical URPs. Second, an application with real measurement data from EEG analysis involving an alpha rhythm is presented, to illustrate the use of URPs on complex-valued narrow band signals in alternative ways. We compare the frequency content on horizontal (or vertical) and on diagonal lines in a URP, and we illustrate how this information can be used to approximate the envelope of the underlying signal.

Section 5 concludes the paper. All the proofs are collected in the Appendix.

2 Unique Reconstruction of a Complex-Valued Signal from Its Unthresholded Recurrence Plot

In this section we extend the results of [1] for real-valued signals, to the class of complex-valued signals $w(t) = x(t) + iy(t)$. Here, $x(t)$ and $y(t)$ denote the real and the imaginary part of $w(t)$, respectively. For a given embedding dimension and time-delay the corresponding trajectories relate similarly as $W(t) = X(t) + iY(t)$. For all time instances u and v it holds that $W(u) \approx W(v)$, i.e., a near recurrence occurs, if and only if both $X(u) \approx X(v)$ and $Y(u) \approx Y(v)$. Therefore, recurrence plots of complex-valued signals are closely related to joint recurrence plots (JRPs), see [14]. To be precise, a *binary* (thresholded) joint recurrence plot is defined as the product of the RPs of the signals $x(t)$ and $y(t)$, which may be constructed for different embedding dimensions, different time-delays and different thresholds:

$$\mathrm{JRP}_{X,Y}^{\varepsilon_X,\varepsilon_Y}(u,v) := \mathrm{RP}_X^{\varepsilon_X}(u,v)\mathrm{RP}_Y^{\varepsilon_Y}(u,v).$$

Note that $\mathrm{URP}_W(u,v)^2 = \|W(u) - W(v)\|^2 = \|X(u) - X(v)\|^2 + \|Y(u) - Y(v)\|^2$. Therefore $\mathrm{RP}_W^{\varepsilon}(u,v) = 1$ if and only if $(\|X(u) - X(v)\|^2 + \|Y(u) - Y(v)\|^2)/\varepsilon^2 \leq 1$, while $\mathrm{JRP}_{X,Y}^{\varepsilon_X,\varepsilon_Y}(u,v) = 1$ if and only if $\max\{\|X(u) - X(v)\|/\varepsilon_X, \|Y(u) - Y(v)\|/\varepsilon_Y\} \leq 1$. This makes clear that the RP of a complex-valued signal employs the 2-norm, while the JRP of two real-valued signals employs a mixture of the

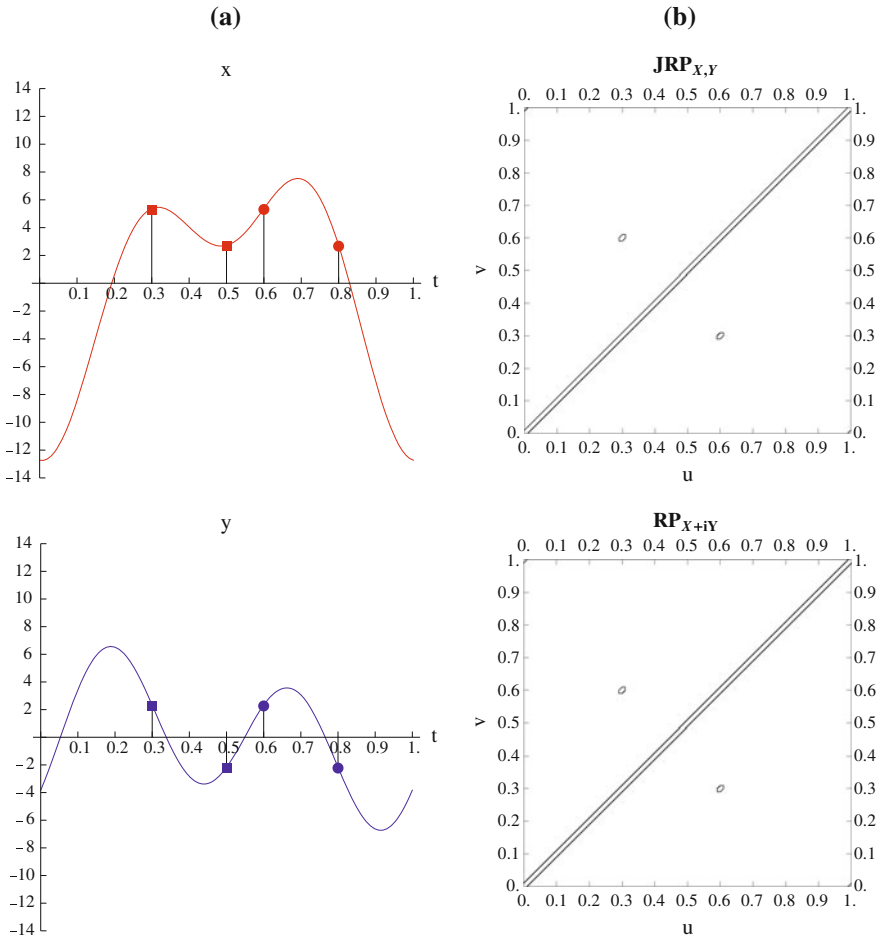

Fig. 1 **a** Real-valued signals $x(t)$ and $y(t)$ with joint recurrences. **b** Joint recurrence plot of $x(t)$ and $y(t)$ (*top*) recurrence plot of the complex-valued signal $w(t) = x(t) + iy(t)$ (*bottom*)

2-norm and the maximum-norm. However, topologically these norms are equivalent (i.e., they define the same families of open sets), so that small distances for one norm correspond to small distances for the other norm. An example of a joint recurrence plot of two real-valued signals and the recurrence plot of the corresponding complex-valued signal for equal embedding dimensions $M = 2$, equal time delays $\tau = 0.2$ and equal thresholds $\varepsilon = 0.1$, is displayed in Fig. 1b. The signal values giving rise to the joint recurrence in $\mathrm{JRP}_{X,Y}(u, v)$ and the recurrence in $\mathrm{RP}_{X+iY}(u, v)$, are indicated by squares and circles in Fig. 1a. The corresponding time instants are $u = 0.3$, $u + \tau = 0.5$, $v = 0.6$ and $v + \tau = 0.8$. This demonstrates that a recurrence plot of a complex-valued signal contains *joint* information on two real-valued signals.

We shall investigate to which extent a recurrence plot of a complex-valued signal also contains *individual* information about the two real-valued signals.

As a URP does not contain information on the mean of a signal, without loss of generality we focus attention on the class of complex-valued zero mean signals $w(t)$. We restrict to signals on $[0, 1)$ which admit a Fourier series representation which converges pointwise almost everywhere and has finite energy:

$$w(t) = \sum_{k\in\mathbb{Z}} w_k e^{2\pi kti}, \quad \text{with } w_0 = 0, \text{ and } \sum_{k\in\mathbb{Z}} |w_k|^2 < \infty. \tag{4}$$

Then for such a signal $w(t)$, for a given embedding dimension M and time-delay τ, the trajectory $W(t)$ is:

$$W(t) = \sum_{k\in\mathbb{Z}} w_k e^{2\pi kti} T_k, \tag{5}$$

in which (for all $k \in \mathbb{Z}$)

$$T_k = \begin{pmatrix} 1 \\ z^k \\ \vdots \\ z^{(M-1)k} \end{pmatrix}, \quad \text{with } z = e^{2\pi\tau i}. \tag{6}$$

When considering the inner product $\langle W(u), W(v)\rangle$ (with linearity in the first argument) as a two-variable function of $u, v \in [0, 1)$, it is obtained that

$$\langle W(u), W(v)\rangle = \sum_{p\in\mathbb{Z}} \sum_{q\in\mathbb{Z}} w_p \overline{w_q} e^{2\pi(pu-qv)i} \langle T_p, T_q\rangle. \tag{7}$$

This constitutes a 2-dimensional Fourier series representation of $\langle W(u), W(v)\rangle$, with 2D-Fourier coefficients $w_p\overline{w_{-q}}\langle T_p, T_{-q}\rangle$. Note that $\langle T_p, T_q\rangle = \langle T_{p+r}, T_{q+r}\rangle$ for all integers p, q, r. An explicit expression for the inner product $\langle T_p, T_q\rangle$ is provided by [1, Lemma 3.1]. It holds that $\langle T_p, T_q\rangle \neq 0$ if and only if $[(p-q)\tau \in \mathbb{Z}] \vee [(p-q)M\tau \notin \mathbb{Z}]$. Also, $\langle T_0, T_0\rangle = M$.

The 2D-Fourier coefficients of $\langle W(u), W(v)\rangle$ enable the computation of the 2D-Fourier coefficients of $\text{URP}_W(u, v)^2$, which are given by the following proposition.

Proposition 1 *Let $w(t) = \sum_{k\in\mathbb{Z}} w_k e^{2\pi kti}$ be a complex-valued zero mean signal from our class. Let $W(t)$ be its trajectory for the embedding dimension M and time-delay τ. Then a 2D-Fourier representation of its squared URP is given by*

$$URP_W(u, v)^2 = \sum_{p\in\mathbb{Z}} \sum_{q\in\mathbb{Z}} \mathscr{W}_{p,q} e^{2\pi(pu+qv)i}, \tag{8}$$

in which the 2D-Fourier coefficients are given by

$$\mathscr{W}_{0,0} = 2M \sum_{k\in\mathbb{Z}} |w_k|^2 \tag{9}$$

$$\mathscr{W}_{p,0} = \langle T_p, T_0\rangle \sum_{k\in\mathbb{Z}} w_{k+p}\overline{w_k} \quad (p \neq 0) \tag{10}$$

$$\mathscr{W}_{0,q} = \langle T_q, T_0\rangle \sum_{k\in\mathbb{Z}} w_{k+q}\overline{w_k} \quad (q \neq 0) \tag{11}$$

$$\mathscr{W}_{p,q} = -\langle T_{p+q}, T_0\rangle \left(w_p\overline{w_{-q}} + \overline{w_{-p}}w_q\right) \quad (p, q \neq 0). \tag{12}$$

Note that $\mathscr{W}_{p,q} = \mathscr{W}_{q,p}$ and $\mathscr{W}_{-p,-q} = \overline{\mathscr{W}_{p,q}}$ for all integers p and q. By choosing $q = -p \neq 0$, it follows that $\mathscr{W}_{p,-p} = -M(|w_p|^2 + |w_{-p}|^2)$. Therefore, when the URPs (for the same time-delay embedding) of two signals with Fourier coefficients $\{w_k\}_{k\in\mathbb{Z}}$ and $\{v_k\}_{k\in\mathbb{Z}}$ happen to coincide, it holds that $|w_p|^2+|w_{-p}|^2 = |v_p|^2+|v_{-p}|^2$ for all $p \in \mathbb{Z}^+$. Observe that $|w_p|^2 + |w_{-p}|^2$ denotes contribution of the frequency p to the power of $w(t)$. Because the 2D-Fourier coefficients of a URP characterize it uniquely, this proves the following result.

Corollary 1 *Let $w(t) = \sum_{k\in\mathbb{Z}} w_k e^{2\pi kti}$ and $v(t) = \sum_{k\in\mathbb{Z}} v_k e^{2\pi kti}$ be two complex-valued zero mean signals from our class. Let $W(t)$ and $V(t)$ be their trajectories, respectively, for the same time-delay embedding. If their URPs coincide, then also the power spectra of the signals $w(t)$ and $v(t)$ coincide. i.e., for all $k \in \mathbb{Z}$ it holds that $|w_k|^2 + |w_{-k}|^2 = |v_k|^2 + |v_{-k}|^2$.*

Sufficient conditions for the reconstruction of a complex-valued signal $w(t)$ from its URP can also be given, in terms of the following associated graph G_W.

Definition 1 Let $w(t) = \sum_{k\in\mathbb{Z}} w_k e^{2\pi kti}$ be a complex-valued zero mean signal from our class. Let $W(t)$ be its trajectory for the embedding dimension M and time-delay τ. Then define the associated graph G_W as the simple undirected graph for which:

(1) the nodes are labeled by positive indices from the set

$$K_W = \{k \in \mathbb{Z}^+ \mid w_k \neq 0 \vee w_{-k} \neq 0\},$$

(2) two distinct nodes labeled $p, q \in K_W$ are adjacent if and only if both $\langle T_p, T_q\rangle \neq 0$ and $\langle T_p, T_{-q}\rangle \neq 0$.

The following theorem contains the main reconstruction result of this section. Note that we will call a graph complete if all nodes are connected to all nodes, including self-loops.

Theorem 1 *Let $w(t) = \sum_{k\in\mathbb{Z}} w_k e^{2\pi kti}$ and $v(t) = \sum_{k\in\mathbb{Z}} v_k e^{2\pi kti}$ be two complex-valued zero mean signals from our class. Let $W(t)$ and $V(t)$ be their trajectories, respectively, for the same time-delay embedding. If the unthresholded recurrence plots URP_W and URP_V coincide and the associated graph G_W is complete, then the signal $v(t)$ is determined by $w(t)$ up to conjugacy and a unimodular factor, i.e., there exists a unimodular constant α such that $v(t) = \alpha w(t)$ or $v(t) = \alpha\overline{w(t)}$.*

Recall that the graph G_W has positively labeled nodes $k \in K_W$ which in fact correspond to the *pairs* of indices $(k, -k)$. Also, adjacency requires both $\langle T_p, T_q \rangle$ and $\langle T_p, T_{-q} \rangle$ to be nonzero. These are more restrictive conditions than what we have used for real-valued signals in [1], where we were able to give necessary and sufficient conditions for the unique reconstruction of a signal from its URP (up to a sign). It is still an open question to find necessary and sufficient conditions for the reconstruction of complex-valued signals.

In the case of a complete graph G_W, Theorem 1 implies that the magnitudes $|v(t)|$ and $|w(t)|$ coincide. This means that a URP with a complete graph uniquely determines the magnitude of the underlying complex-valued signal. On the other hand, if the graph G_W is not complete then signals with magnitudes of different morphology can exhibit identical URPs. The first example of Sect. 4 demonstrates this.

3 Unthresholded Recurrence Plots for Narrow Band Signals

Motivated by practical applications, we now focus on real-valued signals with a *narrow band* power spectrum. A narrow band signal can be considered as an amplitude modulated sinusoid. Due to the special properties of an associated complex signal representation, the well-known 'analytic signal', the results of the previous section can be used to employ unthresholded recurrence plots an alternative way.

Definition 2 For a given real-valued zero mean signal $x(t) = \sum_{k\in\mathbb{Z}} x_k e^{2\pi kti}$, the complex-valued analytic signal $z(t)$ is defined as follows:

$$z(t) = 2\sum_{k>0} x_k e^{2\pi kti}. \tag{13}$$

Consequently: $x(t) = Re\,(z(t))$.

The trajectory $Z(t)$ of the analytic signal $z(t)$ associated with $x(t)$ is given by:

$$Z(t) = 2\sum_{k>0} x_k e^{2\pi kti} T_k. \tag{14}$$

Proposition 2 *Let $z(t) = 2\sum_{k>0} x_k e^{2\pi kti}$ be an analytic signal. Suppose that the squared unthresholded recurrence plot $URP_Z(u, v)^2 = \|Z(u) - Z(v)\|^2$ can be expressed as a 2D-Fourier series:*

$$URP_Z(u, v)^2 = \sum_{p\in\mathbb{Z}}\sum_{q\in\mathbb{Z}} \mathscr{Z}_{p,q} e^{2\pi(pu+qv)i}.$$

Then the 2D-Fourier coefficients $\mathscr{Z}_{p,q}$ can be expressed through the coefficients x_k of the real-valued signal $x(t)$ as:

$$\mathscr{Z}_{m,n} = \begin{cases} -4\langle T_{m+n}, T_0\rangle x_m \overline{x_{-n}} & \text{for } m > 0, n < 0, \\ -4\langle T_{m+n}, T_0\rangle \overline{x_{-m}} x_n & \text{for } m < 0, n > 0, \\ 0 & \text{otherwise.} \end{cases} \tag{15}$$

An analytic signal is a special case of zero mean complex-valued signal $w(t) = \sum_{k\in\mathbb{Z}} w_k e^{2\pi kti}$, with $w_k = 0$ for $k \leq 0$, i.e.: $w(t) = \sum_{k>0} w_k e^{2\pi kti}$. For the class of analytic signals, Corollary 1 therefore reduces to the following result.

Corollary 2 *Let $w(t) = \sum_{k>0} w_k e^{2\pi kti}$ and $v(t) = \sum_{k>0} v_k e^{2\pi kti}$ be two zero mean analytic signals from our class. Let $W(t)$ and $V(t)$ be their trajectories, respectively, for the same time-delay embedding. If their URPs coincide, then also the power spectra of the signals $w(t)$ and $v(t)$ coincide: for all $k > 0$ it holds that $|w_k| = |v_k|$.*

Because the complex conjugate of a nontrivial analytic signal is not itself an analytic signal, Theorem 1 reduces to the following result.

Theorem 2 *Let $w(t) = \sum_{k>0} w_k e^{2\pi kti}$ and $v(t) = \sum_{k>0} v_k e^{2\pi kti}$ be two zero mean analytic signals from our class. Let $W(t)$ and $V(t)$ be their trajectories, respectively, for the same time-delay embedding. If the unthresholded recurrence plots URP_W and URP_V coincide and the associated graph G_W is complete, then the signal $v(t)$ is determined by $w(t)$ up to a unimodular factor, i.e., there exists a unimodular constant α such that $v(t) = \alpha w(t)$.*

We now turn to narrow band analytic signals $z(t)$ which can be regarded as a *amplitude modulated carrier* signals:

$$z(t) = e^{2\pi cti}\left(2x_c + w(t)\right), \tag{16}$$

where $c \in \mathbb{Z}^+$ denotes the index of the corresponding Fourier coefficient x_c and also the *carrier* frequency (which is integer because we consider periodic signals with period 1). The complex-valued signal $w(t) = \sum_{k\in\mathbb{Z}} w_k e^{2\pi kti}$ is referred as the *modulating* signal, which has:

$$w_k = \begin{cases} 2x_{c+k} & \text{for } k > -c \wedge k \neq 0, \\ 0 & \text{for } k \leq -c \text{ or } k = 0. \end{cases} \tag{17}$$

A geometric interpretation of Eq. (16) is given in Fig. 2. There, the narrow band signal $z(t)$ is represented as a rotating vector $\overrightarrow{OQ} = \overrightarrow{OP} + \overrightarrow{PQ}$. The vector $\overrightarrow{OP}$ represents the constant signal $2x_c$ and the vector $\overrightarrow{PQ}$ represents the modulating signal $w(t)$, both rotating at a constant angular velocity $2\pi c$.

The following proposition interrelates the trajectories, the URPs, and the graphs of the analytic signal $z(t)$ and the modulating signal $w(t)$.

Proposition 3 *Let $c \in \mathbb{Z}^+$ be a carrier frequency and $x(t)$ a zero-mean periodic signal from our class. Then:*

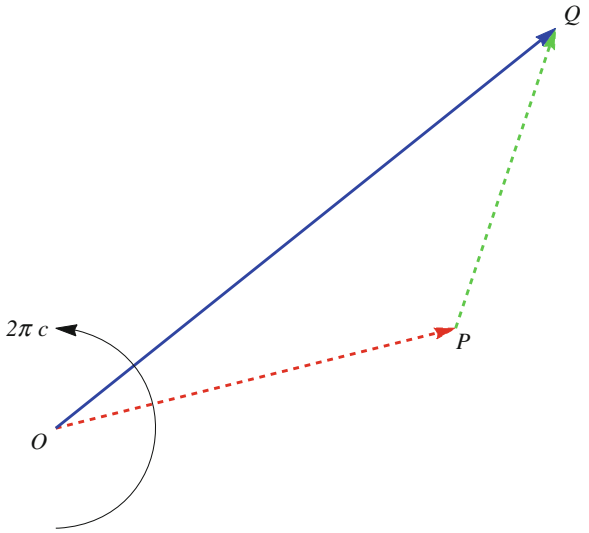

Fig. 2 Geometric interpretation of a narrow band signal $z(t)$ or its trajectory $Z(t)$ as a rotating resultant $\overrightarrow{OQ}$ of a constant vector $\overrightarrow{OP}$ and a modulating vector $\overrightarrow{PQ}$, all rotating at angular velocity $2\pi c$

(1) The trajectory $Z(t)$ of the analytic signal $z(t)$ can be expressed trough the trajectory $W(t)$ of the modulating signal $w(t)$ as:

$$Z(t) = e^{2\pi ct i} diag\,(T_c)\,(2x_c T_0 + W(t))\,. \tag{18}$$

in which $diag(T_c)$ denotes the diagonal matrix having the entries of the vector T_c along its main diagonal.

(2) Let URP_Z and URP_W be the unthresholded recurrence plots of the analytic signal $z(t)$ and the modulating signal $w(t)$, respectively. If $c(u-v) \in \mathbb{Z}$ then:

$$|Z(u) - Z(v)| = |W(u) - W(v)|\,, \tag{19}$$

$$URP_Z(u,v) = URP_W(u,v), \tag{20}$$

in which $|\cdot|$ denotes the entry-wise absolute value.

(3) The 2D-Fourier coefficients $\mathscr{W}_{p,q}$ of $URP_W(u,v)^2$ can be expressed through the 2D-Fourier coefficients $\mathscr{Z}_{p,q}$ of $URP_Z(u,v)^2$ as:

$$\mathscr{W}_{p,q} = \mathscr{Z}_{p+c,q-c} + \mathscr{Z}_{q+c,p-c}. \tag{21}$$

(4) The nodes of the graph G_W can be obtained from the nodes of the graph G_Z as:

$$K_W = \{k \in \mathbb{Z}^+ \,|\, x_{c+k} \neq 0 \vee x_{c-k} \neq 0\}. \tag{22}$$

Figure 2 also provides a geometric interpretation of part (1) of this proposition. Now, the trajectory $Z(t)$ is represented as a rotating vector $\overrightarrow{OQ} = \overrightarrow{OP} + \overrightarrow{PQ}$, rotating at a constant angular velocity $2\pi c$. The vectors $\overrightarrow{OP}$ and $\overrightarrow{PQ}$ now represent the constant vector diag (T_c) $(2x_c T_0) = 2x_c T_c$ and the modulating trajectory diag (T_c) $W(t)$, respectively.

In order to go beyond the visual impression yielded by RPs, several measures which quantify structures in RPs, have been proposed in [3] and are known as recurrence quantification analysis (RQA). These measures are based on *horizontal* (or *vertical*) and on *diagonal* lines of an RP. An important difference between the unthresholded recurrence plots URP_X^2 and URP_Z^2 for narrow band signals lies in the frequency content of their restrictions to these lines.

Since we consider complex-valued periodic signals with period $T = 1$ it holds that $f_k = \frac{k}{T} = k$. Therefore, for convenience we shall call the indices k also frequencies.

Proposition 4 *Let $x(t)$ be a zero-mean real periodic signal with period 1, which has a finite Fourier series with the frequency range $\{c-d, \ldots, c+d\}$. Then:*

(1) The restrictions of $URP_X(u,v)^2$ to horizontal, vertical and diagonal lines, have the frequency ranges:

$$\begin{array}{ll} v & \text{is constant} : \{0, \ldots, 2d\} \cup \{c-d, \ldots, c+d\} \cup \{2c-2d, \ldots, 2c+2d\}; \\ u & \text{is constant} : \{0, \ldots, 2d\} \cup \{c-d, \ldots, c+d\} \cup \{2c-2d, \ldots, 2c+2d\}; \\ u-v & \text{is constant} : \{0, \ldots, 2d\} \cup \{2c-2d, \ldots, 2c+2d\}. \end{array}$$

(2) The restrictions of $URP_Z(u,v)^2$ to horizontal, vertical and diagonal lines, have the frequency ranges:

$$\begin{array}{ll} v & \text{is constant} : \{0, \ldots, 2d\} \cup \{c-d, \ldots, c+d\}; \\ u & \text{is constant} : \{0, \ldots, 2d\} \cup \{c-d, \ldots, c+d\}; \\ u-v & \text{is constant} : \{0, \ldots, 2d\}. \end{array}$$

(3) The frequency ranges $\{0, \ldots, 2d\}$, $\{c-d, \ldots, c+d\}$ and $\{2c-2d, \ldots, 2c+2d\}$ are mutually disjoint if and only if $c > 3d$.

Note that, contrary to $\text{URP}_X(u,v)^2$, the restrictions of $\text{URP}_Z(u,v)^2$ to horizontal, vertical and diagonal lines, have no frequencies in the range $\{2c-2d, \ldots, 2c+2d\}$. Also note that the frequency range of the restriction of $\text{URP}_Z(u,v)^2$ to diagonal lines only depends on the bandwidth $2d$ of the signal $x(t)$. These properties appear as *elongated* contours along the diagonal lines in URP_Z.

To illustrate this result, we here present an example. We consider a real signal $x(t) = \sum_{k=-22}^{-18} x_k e^{2\pi kti} + \sum_{k=18}^{22} x_k e^{2\pi kti}$, involving just five different frequencies, for which the Fourier coefficients are given by:

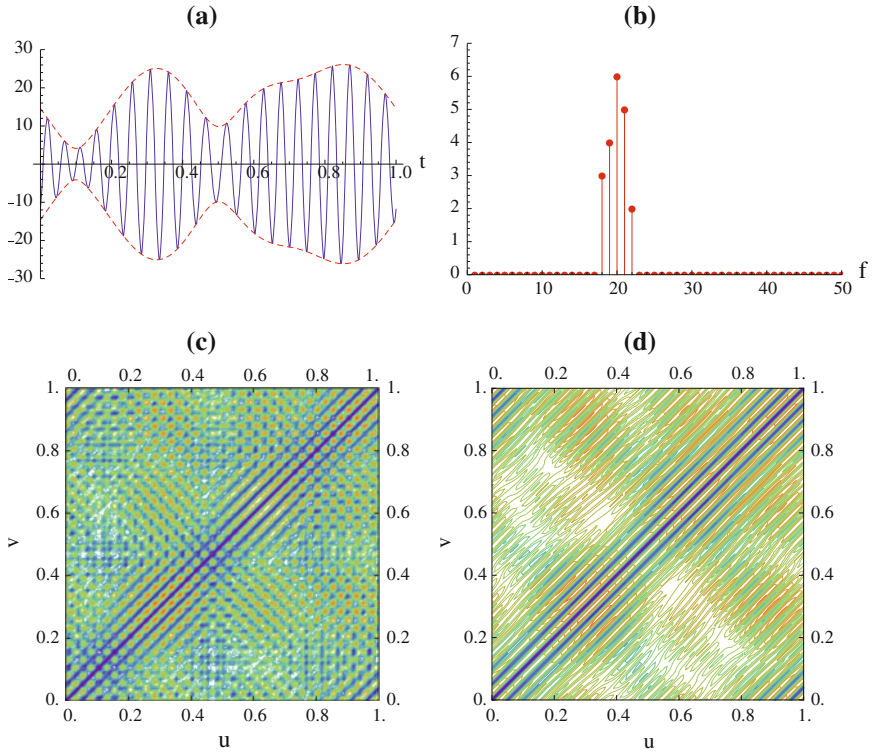

Fig. 3 **a** Signal $x(t)$ and its envelope $\pm|z(t)|$, **b** magnitude spectrum of $x(t)$, **c** URP of the real signal $x(t)$, **d** URP of the analytic signal $z(t)$

$$
\begin{aligned}
x_{18} &= \overline{x_{-18}} = 3e^{-5i},\\
x_{9} &= \overline{x_{-9}} = 4e^{3i},\\
x_{10} &= \overline{x_{-10}} = 6e^{4i},\\
x_{11} &= \overline{x_{-11}} = 5e^{-2i},\\
x_{22} &= \overline{x_{-22}} = 2e^{-6i}.
\end{aligned}
$$

The signal $x(t)$ and its analytic signal $z(t)$ have the frequency range $\{c-d, \ldots, c+d\}$ for the settings $c = 20$ and $d = 2$. The signal $x(t)$ and its *envelope* $\pm|z(t)|$ are displayed in Fig. 3a. The magnitude spectrum of $x(t)$ is displayed in Fig. 3b. The unthresholded recurrence plots URP_X and URP_Z are computed for the settings $M = 4$ and $\tau = \frac{1}{3}$ and are displayed in Fig. 3c and d, respectively. The magnitude spectra of $\mathrm{URP}_X(u,v)^2$ and $\mathrm{URP}_Z(u,v)^2$ on the horizontal lines $(u,v) = (t, 0.625)$, the vertical lines $(u,v) = (0.625, t)$ and on the diagonal lines $(u,v) = (t + 0.125, t)$, with $t \in [0, 1)$, are displayed in Fig. 4a and b, respectively. These figures demonstrate that different parts of the spectrum can be investigated in isolation, by studying appropriately selected lines in the URPs of either $x(t)$ or $z(t)$.

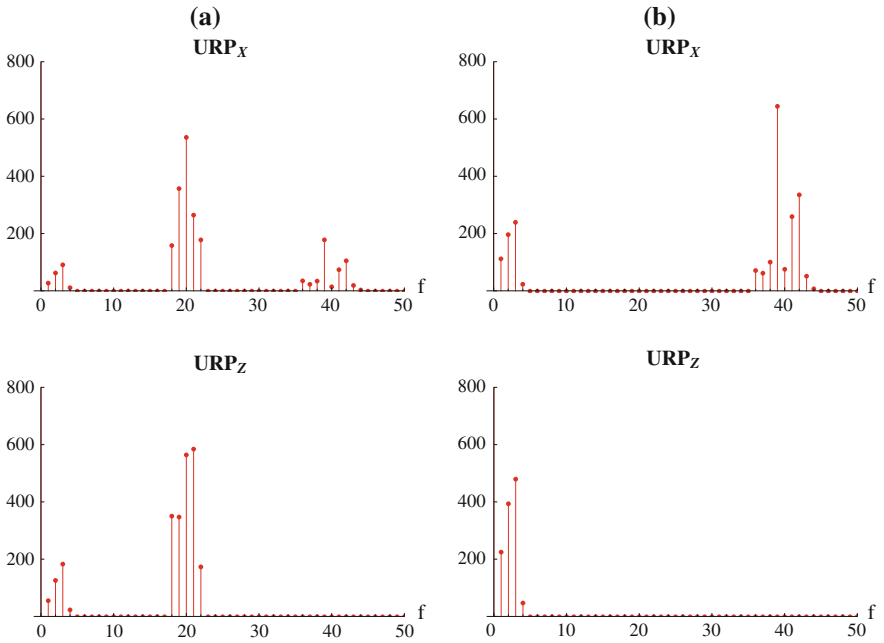

Fig. 4 Magnitude spectra along selected lines [**a** $u = 0.625$ or $v = 0.625$, **b** $u - v = 0.125$] in the squared URPs of the signal $x(t)$ (*top*) and its analytic signal $z(t)$ (*bottom*)

4 Examples, Including an Application in EEG Analysis

To illustrate the main results and techniques of the previous sections, we here present two more examples.

In the first example we investigate four different settings for M and τ, which may cause complex-valued signals with morphologically different magnitudes still to exhibit identical URPs. This example serves to demonstrate the limitations that apply to the interpretation of a URP, emanating from the choice of embedding dimension and time-delay.

In the second example we consider an application in EEG analysis, which concerns a digitally sampled measurement signal featuring a so-called alpha rhythm. The measured alpha rhythm is band-pass filtered to obtain the so-called alpha band signal. We investigate the unthresholded recurrence plots of the associated analytic signal and the modulating signal for a given choice of the carrier frequency.

Example 1 Different complex-valued signals exhibiting identical URPs. For four different settings of M and τ we give pairs of complex-valued signals $v(t) = \sum_{k=-2}^{2} v_k e^{2\pi k t i}$, $w(t) = \sum_{k=-2}^{2} w_k e^{2\pi k t i}$ with morphologically different magnitudes but identical URPs. In accordance with Corollary 1 it holds that $|v_{-k}|^2 + |v_k|^2 = |w_{-k}|^2 + |w_k|^2$, for $k \in 1, 2$.

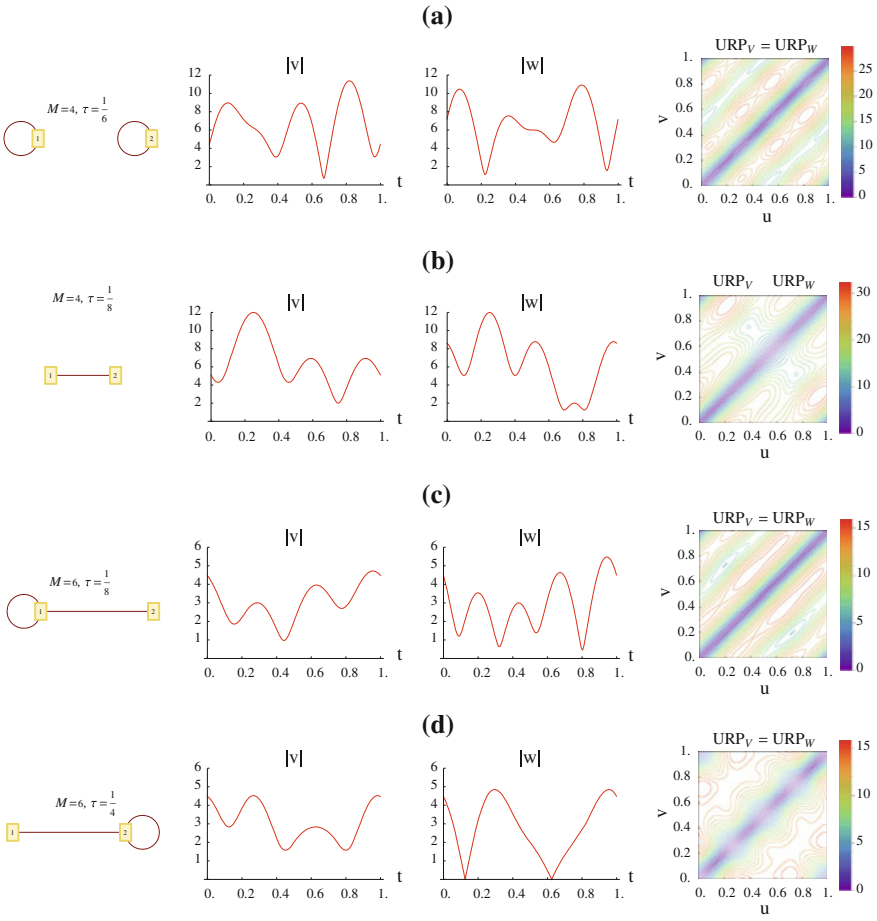

Fig. 5 Graphs, magnitudes and URPs for different settings of embedding dimension M and time-delay τ, for four different pairs of signals $v(t)$ and $w(t)$ specified in the text

The associated graphs G_V and G_W in all cases have exactly 2 nodes, labeled 1 and 2. Adjacency of those nodes depends on the values of M and τ. Recall that two distinct nodes $p, q \in K_W$ are adjacent if and only if both $\langle T_p, T_q \rangle \neq 0$ and $\langle T_p, T_{-q} \rangle \neq 0$.

(i) $M = 4$ and $\tau = \frac{1}{6}$, see Fig. 5a.

$$v_{-2} = 6, \quad v_{-1} = 1, \quad v_1 = -3, \; v_2 = -2i,$$
$$w_{-2} = 6i, \; w_{-1} = -1, \; w_1 = 3, \quad w_2 = 2.$$

The graph is not complete, since the nodes 1 and 2 are not adjacent.

(ii) $M = 4$ and $\tau = \frac{1}{8}$, see Fig. 5b.

$$v_{-2} = 0,\ v_{-1} = 3,\ v_1 = -4,\ v_2 = 5i,$$
$$w_{-2} = 3,\ w_{-1} = 0,\ w_1 = 5i,\ w_2 = 4.$$

The graph is not complete, since the nodes 1 and 2 both have no self-loops.

(iii) $M = 6$ and $\tau = \frac{1}{8}$, see Fig. 5c.

$$v_{-2} = 0,\quad v_{-1} = 1,\ v_1 = 1,\ v_2 = 2 + 2i,$$
$$w_{-2} = -2i,\ w_{-1} = 1,\ w_1 = 1,\ w_2 = 2.$$

The graph is not complete, since the node 2 has no self-loop.

(iv) $M = 6$ and $\tau = \frac{1}{4}$, see Fig. 5d.

$$v_{-2} = 1,\ v_{-1} = 0,\quad v_1 = 2 + 2i,\ v_2 = 1,$$
$$w_{-2} = 1,\ w_{-1} = -2i,\ w_1 = 2,\quad w_2 = 1.$$

The graph is not complete, since the node 1 has no self-loop.

This example demonstrates that for certain 'unfortunate' choices of M and τ the magnitude of the underlying complex-valued signal cannot be uniquely retrieved from the URP. In such cases, in view of Theorem 1, the graphs associated with the URPs are incomplete.

Example 2 EEG analysis featuring an alpha rhythm. In EEG analysis an EEG signal is decomposed into five band signals corresponding to the delta (0.1–4 Hz), theta (4–8 Hz), alpha (8–12 Hz), beta (12–30 Hz), and gamma (30–100 Hz) frequency bands, see [15]. These basic EEG frequency bands are understood to reflect different functional processes in the brain.

From a digitally sampled EEG measurement signal we consider an excerpt of $N = 500$ samples, exhibiting an alpha rhythm, with a duration of $T = 2$ s. Alpha rhythms are characterized by a clear peak in their magnitude spectrum for a frequency in the alpha band (8–12 Hz), see Fig. 6a. The alpha band signal $x(t)$, see Fig. 6b, is obtained from the alpha rhythm by selecting the coefficients with frequencies $f_k = \frac{k}{T}$ in the alpha frequency band, i.e. $k \in \{16, \ldots, 24\}$. For the setting $c = 20$ (i.e. $f_c = \frac{c}{T}$ = 10 Hz), the modulating signal $w(t)$ is constructed from the analytic signal $z(t)$ using Eq. (16). The URPs of the signal $z(t)$ and the signal $w(t)$, for the settings $M = 3$ and $\tau = \frac{1}{50}T = 0.04$ s, are both displayed in Fig. 7. Note that τ is an integer multiple of the sampling time $\Delta t := \frac{T}{N} = 0.004$ s.

The graph G_Z has 9 nodes: $k \in K_Z = \{16, \ldots, 24\}$. The graph G_W has 4 nodes: $k \in K_W = \{1, \ldots, 4\}$ which are obtained from K_Z by using part (4) of Proposition 3. Since M and the denominator of $\frac{\tau}{T}$ are co-prime, it follows from Part (2) of [1, Corollary 3.5] that the graphs G_Z and G_W are complete. Consequently, the signal $z(t)$ is determined up to a unimodular factor by URP_Z, and the signal $w(t)$ is determined up to conjugacy and a unimodular factor by URP_W.

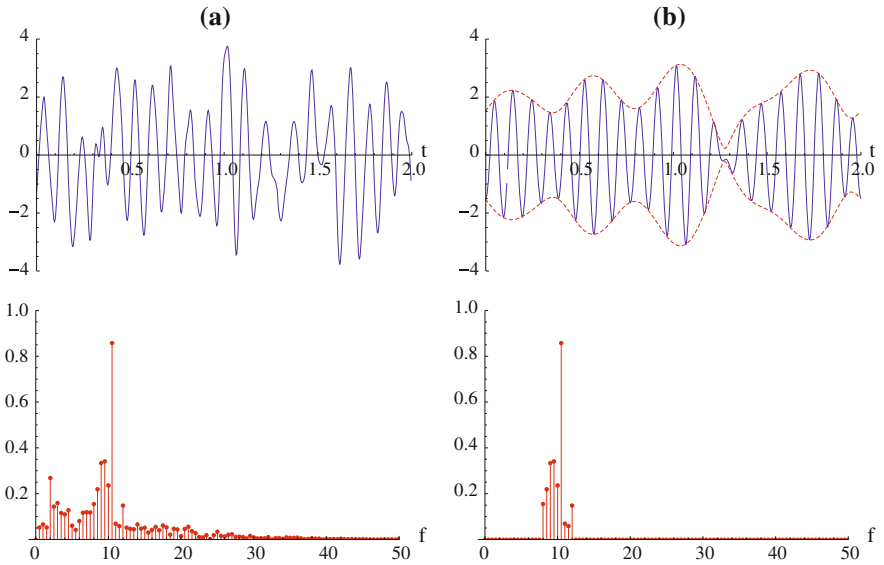

Fig. 6 **a** Measured alpha rhythm signal (*top*), **b** selected alpha band signal (*top*), and their corresponding magnitude spectra (*bottom*)

According to part (1) of Proposition 3 it holds that $\mathrm{URP}_Z(u,v)$ an $\mathrm{URP}_W(u,v)$ coincide on the diagonal lines $10(u-v) \in \mathbb{Z}$, but they are different between these lines. Some of these diagonal lines are indicated by dashed black lines in the upper triangular part of URP_W, see in Fig. 7. In view of part (2) of Proposition 4 it holds that the signals $z(t)$ and $w(t)$ have frequency ranges $\{\frac{k}{T} \mid |k| \in \{c-d,\ldots,c+d\}\}$ and $\{\frac{k}{T} \mid |k| \in \{1,\ldots,d\}\}$, respectively, for the settings $c = 20$ and $d = 4$. Therefore the restrictions of $\mathrm{URP}_W(u,v)^2$ to horizontal, vertical and diagonal lines, all have the frequency range $\{\frac{k}{T} \mid |k| \in \{0,\ldots,2d\}\} = \{\frac{k}{2} \mid |k| \in \{0,\ldots,8\}\}$. The restriction of $\mathrm{URP}_Z(u,v)^2$ diagonal lines has the latter frequency range too, whereas the restrictions to horizontal and vertical lines also have *higher* frequencies in the range $\{\frac{k}{T} \mid |k| \in \{c-d,\ldots,c+d\}\} = \{\frac{k}{2} \mid |k| \in \{16,\ldots,24\}\}$.

In EEG amplitude modulation analysis, the envelopes of EEG band signals are studied, see e.g. [16–20]. In this example, the envelope $\pm|z(t)|$ of the alpha band signal $x(t)$ is displayed in Fig. 6b. The horizontal and vertical lines in URP_Z provide information about the magnitude $|z(t)|$. To illustrate this, we approximate $|z(t)|$ by $\sqrt{\frac{|z(t-\tau)|^2+|z(t)|^2+|z(t+\tau)|^2}{3}} = \frac{\|Z(t-\frac{1}{2}(M-1)\tau)\|}{\sqrt{M}}$. The norm $\|Z(t-\frac{1}{2}(M-1)\tau)\|$ in the latter term can be computed by using an identity provided by [1, Proposition 5.1]:

$$T^2\|Z(t)\|^2 = T\int_0^T \mathrm{URP}_Z(u,t)^2\,du - \frac{1}{2}\int_0^T\int_0^T \mathrm{URP}_Z(u,v)^2\,du\,dv. \qquad (23)$$

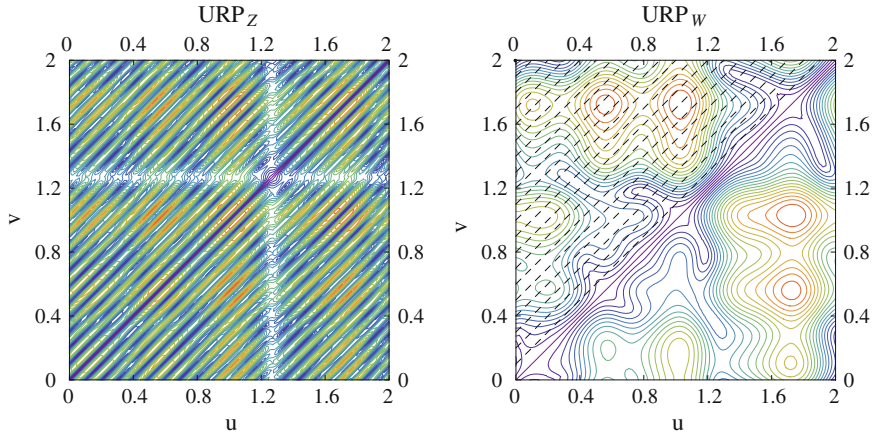

Fig. 7 URPs of the analytical signal $z(t)$ and the modulating signal $w(t)$

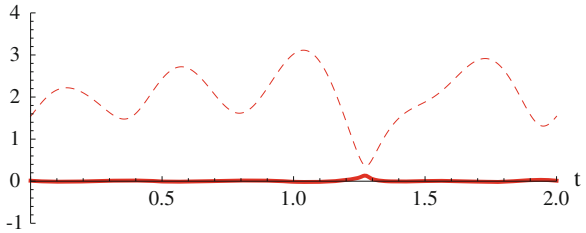

Fig. 8 Approximation for the envelope $|z(t)|$ (*dashed*) constructed from horizontal lines in URP$_Z$, and the corresponding approximation error (*solid*)

The integrand in the single integral term is a restriction of URP$_Z$ to the horizontal line corresponding to a given time instance t. The double integral has a constant value which is independent of t. The approximation $\frac{\|Z(t-\frac{1}{2}(M-1)\tau)\|}{\sqrt{M}}$ (dashed graph) and the approximation error $\frac{\|Z(t-\frac{1}{2}(M-1)\tau)\|}{\sqrt{M}} - |z(t)|$ (solid graph) are displayed in Fig. 8. This example shows how the frequency range of the complex-valued modulating signal $w(t)$ can be determined from the frequency range of the restrictions of URP$_Z^2$ to diagonal lines. It also demonstrates how the envelope of the real-valued narrow band signal $x(t)$ is related to the information content of the horizontal and vertical lines in URP$_Z$. As a new alternative method for EEG amplitude modulation analysis one could study URP$_W$ instead.

5 Conclusions and Discussion

When considering URPs as a tool to extract information from complex-valued signals, we have argued in this paper that it is important to first establish which information can or cannot be recovered from URPs.

In Sect. 2 we extended our work [1], concerning URPs of real-valued signals, to complex-valued signals. There we focused on computing the Fourier coefficients w_k of $w(t)$ from the 2D-Fourier coefficients $\mathscr{W}_{p,q}$ of URP_W. We showed that a signal $w(t)$, with a complete associated graph G_W, can be uniquely recovered from its URP up to conjugacy and a unimodular factor, see Theorem 1. If the graph G_W is not complete then signals with morphologically different magnitudes can exhibit identical URPs. The first example of Sect. 4 demonstrates this. We also related recurrence plots of complex-valued signals to *joint recurrence plots* which allows studying the relationship between two real-valued signals, see [14]. It is found that recurrence plots of complex-valued signals can be used to locate joint recurrences in a pairs of real-valued signals.

In Sect. 3, we used the special properties of *complex signal representation* to study signals with a narrow band power spectrum. For a given choice of the carrier frequency, a corresponding modulating signal can be computed from the analytic signal. Modulating signals provide an alternative way to employ URPs for studying narrow band signals. The trajectories, URPs and the graphs of the analytic signal and the modulating signal are related in Proposition 3. The frequency ranges of restrictions of a URP on horizontal, vertical and diagonal lines are investigated to explain the elongated contours along the diagonal lines in the URP of the analytic signal. It is shown how the frequency range of restrictions on horizontal and vertical lines differs from that on diagonal lines. It is found how the frequency ranges of these restrictions for a real-valued signal differ from those of the corresponding analytic signal. We also illustrated how the information content on horizontal and vertical lines in a URP can be used to approximate the envelope of the underlying narrow band signal. These results are demonstrated by the second example of Sect. 4.

A couple of research questions still remain open. (1) One important question concerns redundancy in the URP, being a 2-dimensional representation of a 1-dimensional signal, which is currently under investigation. The question arises to which extent a selected part of a URP may still contain all the information contained in the entire URP. This is of importance for relating subpatterns in a unthresholded recurrence plot URP_W to localized (morphological) properties of the underlying complex-valued signal $w(t)$. (2) To quantify patterns that occur in RPs, several measures have been proposed in the literature, see e.g. [3], that are used in recurrence quantification analysis (RQA). An important question concerns the generalization of these measures to RPs of complex-valued signals.

Acknowledgments This research is conducted in collaboration with and supported by BrainMarker BV, the Netherlands, in the course of its development of a decision support system for EEG based brain state analysis.

Appendix

Proof of Proposition 1 Observe that

$$\|W(u) - W(v)\|^2 = \|W(u)\|^2 - \langle W(u), W(v)\rangle - \langle W(v), W(u)\rangle + \|W(v)\|^2.$$

For arbitrary t we have:

$$\begin{aligned}\|W(t)\|^2 &= \sum_{p\in\mathbb{Z}}\sum_{q\in\mathbb{Z}} w_p\overline{w_q}\langle T_p, T_q\rangle e^{2\pi(p-q)ti} = \sum_{k\in\mathbb{Z}}\sum_{q\in\mathbb{Z}} w_{q+k}\overline{w_q}\langle T_k, T_0\rangle e^{2\pi kti}\\ &= \sum_{k\in\mathbb{Z}}\langle T_k, T_0\rangle e^{2\pi kti}\sum_{q\in\mathbb{Z}} w_{k+q}\overline{w_q}.\end{aligned}$$

For $t = u$ and $t = v$ this specializes to:

$$\begin{aligned}\|W(u)\|^2 &= \sum_{p\in\mathbb{Z}}\langle T_p, T_0\rangle e^{2\pi pui}\sum_{k\in\mathbb{Z}} w_{k+p}\overline{w_k},\\ \|W(v)\|^2 &= \sum_{q\in\mathbb{Z}}\langle T_q, T_0\rangle e^{2\pi qvi}\sum_{k\in\mathbb{Z}} w_{k+q}\overline{w_k}.\end{aligned}$$

For $\langle W(u), W(v)\rangle$ we have already presented the expression

$$\begin{aligned}\langle W(u), W(v)\rangle &= \sum_{p\in\mathbb{Z}}\sum_{q\in\mathbb{Z}} w_p\overline{w_q}\langle T_p, T_q\rangle e^{2\pi(pu-qv)i}\\ &= \sum_{p\in\mathbb{Z}}\sum_{q\in\mathbb{Z}} w_p\overline{w_{-q}}\langle T_{p+q}, T_0\rangle e^{2\pi(pu+qv)i}.\end{aligned}$$

It follows that

$$\langle W(u), W(v)\rangle + \langle W(v), W(u)\rangle = \sum_{p\in\mathbb{Z}}\sum_{q\in\mathbb{Z}}\langle T_{p+q}, T_0\rangle\left(w_p\overline{w_{-q}} + \overline{w_{-p}}w_q\right)e^{2\pi(pu+qv)i}.$$

Using $w_0 = 0$, it follows for $p = q = 0$ that:

$$\mathscr{W}_{0,0} = 2M\sum_{k\in\mathbb{Z}}|w_k|^2.$$

For $p \neq 0, q = 0$:

$$\mathscr{W}_{p,0} = \langle T_p, T_0\rangle\sum_{k\in\mathbb{Z}} w_{k+p}\overline{w_k}.$$

For $p = 0, q \neq 0$:

$$\mathscr{W}_{0,q} = \langle T_q, T_0 \rangle \sum_{k\in\mathbb{Z}} w_{k+q}\overline{w_k}.$$

And for $p \neq 0, q \neq 0$:

$$\mathscr{W}_{p,q} = -\langle T_{p+q}, T_0 \rangle (w_p \overline{w_{-q}} + \overline{w_{-p}} w_q). \tag{24}$$

□

Proof of Theorem 1 First observe that the URPs for $w(t)$ and $v(t)$ coincide if and only of their 2D-Fourier representations coincide. This requires that

$$\begin{aligned}
&\sum_{k\in\mathbb{Z}} |w_k|^2 = \sum_{k\in\mathbb{Z}} |v_k|^2,\\
&\langle T_p, T_0 \rangle \sum_{k\in\mathbb{Z}} w_{k+p}\overline{w_k} = \langle T_p, T_0 \rangle \sum_{k\in\mathbb{Z}} v_{k+p}\overline{v_k}, \quad \text{for all } p \neq 0,\\
&\langle T_{p+q}, T_0 \rangle (w_p \overline{w_{-q}} + \overline{w_{-p}} w_q) = \langle T_{p+q}, T_0 \rangle (v_p \overline{v_{-q}} + \overline{v_{-p}} v_q), \quad \text{for all } p, q \neq 0.
\end{aligned}$$

As we have seen, choosing $q = -p \neq 0$ in the third of these conditions implies that: $|w_p|^2 + |w_{-p}|^2 = |v_p|^2 + |v_{-p}|^2$ for all $p \in \mathbb{Z}^+$. Summation over all p then implies the first of these conditions. Likewise, choosing $p = k + \tilde{p}$ and $q = -k$ in the third of these conditions gives: $\langle T_{\tilde{p}}, T_0 \rangle (w_{k+\tilde{p}} \overline{w_k} + \overline{w_{-k+\tilde{p}}} w_{-k}) = \langle T_{\tilde{p}}, T_0 \rangle (v_{k+\tilde{p}} \overline{v_k} + \overline{v_{-k+\tilde{p}}} v_{-k})$. Summation over all $k \in \mathbb{Z}$ now implies the second of these conditions. Therefore, the two URPs coincide if and only if the third condition holds.

To address this condition, a special subclass of 2×2 complex matrices is introduced. For all $\alpha, \beta \in \mathbb{C}$ define the associated matrices $S(\alpha, \beta)$ as:

$$S(\alpha, \beta) = \begin{pmatrix} \alpha & \overline{\beta} \\ \beta & \overline{\alpha} \end{pmatrix}.$$

For this subclass, note that $S(\alpha, \beta)S(\gamma, \delta) = S(\alpha\gamma + \overline{\beta}\delta, \overline{\alpha}\delta + \beta\gamma)$ and $\det S(\alpha, \beta) = |\alpha|^2 - |\beta|^2$. It follows that the subclass of invertible matrices $S(\alpha, \beta)$ forms a multiplicative group (under ordinary matrix multiplication), with $S(\alpha, \beta)^{-1} = S(\frac{\overline{\alpha}}{|\alpha|^2 - |\beta|^2}, \frac{-\beta}{|\alpha|^2 - |\beta|^2})$. The intersection of this group with the group of unitary matrices (for which inversion coincides with Hermitian transposition) consists of the matrices $S(\alpha, \beta)$ with $|\alpha|^2 + |\beta|^2 = 1$ and $\alpha\beta = 0$ (i.e., either $\alpha = 0$ and $|\beta| = 1$, or $|\alpha| = 1$ and $\beta = 0$).

The usefulness of this matrix group lies in the observation that two identities

$$\begin{aligned}
\mathscr{W}_{p,-q} &= -\langle T_{p-q}, T_0 \rangle (w_p \overline{w_q} + \overline{w_{-p}} w_{-q})\\
\mathscr{W}_{-p,-q} &= -\langle T_{-p-q}, T_0 \rangle (w_{-p} \overline{w_q} + \overline{w_p} w_{-q})
\end{aligned}$$

are jointly captured by the matrix identity

$$S(w_p, w_{-p})S(w_q, w_{-q})^* = -S\left(\frac{\mathscr{W}_{p,-q}}{\langle T_{p-q}, T_0\rangle}, \frac{\mathscr{W}_{-p,-q}}{\langle T_{-p-q}, T_0\rangle}\right), \tag{25}$$

provided that $\langle T_{p-q}, T_0\rangle$ and $\langle T_{-p-q}, T_0\rangle$ are both nonzero. When p and q are adjacent nodes in the graph G_W, this condition holds; this is implied by the completeness assumption for the graph G_W. Then the corresponding 2D-Fourier coefficients $\mathscr{W}_{p,-q}$ and $\mathscr{W}_{-p,-q}$ coincide with their counterparts $\mathscr{V}_{p,-q}$ and $\mathscr{V}_{-p,-q}$, respectively, if and only if

$$S(w_p, w_{-p})S(w_q, w_{-q})^* = S(v_p, v_{-p})S(v_q, v_{-q})^*.$$

We consider two different cases.

(a) Suppose that $|w_p| \neq |w_{-p}|$ for some $p \in K_W$. Then $S(w_p, w_{-p})$ is invertible. Upon choosing $q = p$, we have that $S(w_p, w_{-p})S(w_p, w_{-p})^* = S(v_p, v_{-p})$ $S(v_p, v_{-p})^*$ can be rewritten as $S(w_p, w_{-p})^{-1}S(v_p, v_{-p})S(v_p, v_{-p})^*$ $S(w_p, w_{-p})^{-*} = I$. Therefore: $S(v_p, v_{-p}) = S(w_p, w_{-p})S(\alpha, \beta)$ for some unitary matrix $S(\alpha, \beta)$. For the choice $q \neq p$, we then have that $S(w_p, w_{-p})$ $S(w_q, w_{-q})^* = S(v_p, v_{-p})S(v_q, v_{-q})^*$ becomes equivalent to $S(v_q, v_{-q}) = S(w_q, w_{-q})S(\alpha, \beta)$, involving the same unitary matrix $S(\alpha, \beta)$. Now it is easily verified that if $\alpha = 0$ then $v_q = \beta w_{-q}$ for all $q \in K_W$, i.e.: $v(t) = \beta\overline{w(t)}$ for a unimodular constant β. Alternatively, if $\beta = 0$ then $v_q = \alpha w_q$ for all $q \in K_W$, i.e.: $v(t) = \alpha w(t)$ for a unimodular constant α.

(b) Suppose that $|w_p| = |w_{-p}|$ for all $p \in K_W$. Then for the choices $p = -q = k$ and $p = q = k$ we obtain the two conditions:

$$|w_k|^2 + |w_{-k}|^2 = |v_k|^2 + |v_{-k}|^2,$$
$$w_k\overline{w_{-k}} = v_k\overline{v_{-k}}.$$

It follows that $v_k = u_k w_k$ and $v_{-k} = u_k w_{-k}$ for some unimodular factor u_k. Then the normalized (unimodular) quantities $V_k := \frac{v_k}{|v_k|}$ and $W_k := \frac{w_k}{|w_k|}$ satisfy $V_k = u_k W_k$, $V_{-k} = u_k W_{-k}$ and $V_p\overline{V_{-q}} + \overline{V_{-p}}V_q = W_p\overline{W_{-q}} + \overline{W_{-p}}W_q$. Hence: $\left(\frac{u_p}{u_q} - 1\right)\left(\frac{u_p}{u_q} - \frac{W_q W_{-q}}{W_p W_{-p}}\right) = 0$ if and only if $u_p = u_q$ or $u_p W_p W_{-p} = u_q W_q W_{-q}$.

First, suppose $W_m W_{-m} \neq W_n W_{-n}$ and $u_m = u_n$ for some $m, n \in K_W$. For $k \in K_W$ we have $u_k = u_m$ or $u_k W_k W_{-k} = u_m W_m W_{-m}$. Similarly, it holds that $u_k = u_n$ or $u_k W_k W_{-k} = u_n W_n W_{-n}$. Since $u_k W_k W_{-k} = u_m W_m W_{-m}$ and $u_k W_k W_{-k} = u_n W_n W_{-n}$ cannot both hold true, it follows that $u_k = u_m$ or $u_k = u_n$. This implies that for all $k \in K_W$: $u_k = \alpha$ for some unimodular constant α. Hence $V_k = \alpha W_k$ for all k if and only if $v_k = \alpha w_k$ for all k, which holds if and only if $v(t) = \alpha w(t)$.

Otherwise, suppose $u_m \neq u_n$. Again, for $k \in K_W$ we have $u_k = u_m$ or $u_k W_k W_{-k} = u_m W_m W_{-m}$. Similarly, it holds that $u_k = u_n$ or $u_k W_k W_{-k} = u_n W_n W_{-n}$. Since $u_k = u_m$ and $u_k = u_n$ cannot both hold true it follows that $u_k W_k W_{-k} = u_m W_m W_{-m}$ or $u_k W_k W_{-k} = u_n W_n W_{-n}$. This implies that for all $k \in K_W$: $u_k W_k W_{-k} = u_m W_m W_{-m} = u_n W_n W_{-n} = \beta$ for some unimodular constant β. Hence $u_k W_k W_{-k} = u_p W_p W_{-p} = u_q W_q W_{-q} = \beta$ for some unimodular

constant β. Therefore $V_k = \beta\overline{W_{-k}}$ for all k if and only if $v_k = \beta\overline{w_{-k}}$ for all k, if and only if $v(t) = \beta\overline{w(t)}$.

Finally, suppose $W_m W_{-m} = W_n W_{-n}$ for all $m, n \in K_W$. Then $u_k = u_n$ or $u_k W_k W_{-k} = u_n W_n W_{-n}$ implies $u_k = u_n$. Hence, for all $k \in K_W$: $u_k = \alpha$ for some unimodular constant α. Therefore $V_k = \alpha W_k$ for all k if and only if $v_k = \alpha w_k$ for all k, if and only if $v(t) = \alpha w(t)$.

□

Proof of Proposition 3

(1) From Eq. (16) we have that:

$$z(t + m\tau) = e^{2\pi c(t+m\tau)i}\,(2x_c + w(t + m\tau)) = e^{2\pi cti}e^{2\pi cm\tau i}\,(2x_c + w(t + m\tau))$$

In this expression, the factor $e^{2\pi cm\tau i}$ is the $(m + 1)$-th diagonal entry of the matrix $diag(T_c)$. The factor $2x_c + w(t + m\tau)$ is the $(m+1)$-th entry of the vector $2x_c T_0 + W(t)$.

(2) Suppose $c(u - v) \in \mathbb{Z}$, then $e^{2\pi cui} = e^{2\pi cvi}$. Hence $Z(u) - Z(v) = e^{2\pi cui}\,\mathrm{diag}\,(T_c)\,(Z(u) - Z(v))$, which implies that $|Z(u) - Z(v)| = |W(u) - W(v)|$ and $\|Z(u) - Z(v)\| = \|W(u) - W(v)\|$.

(3) First, suppose $m = c + p > 0$ and $n = q - c < 0$. Then, from Proposition 2 and Eq. (17) it follows that:

$$\mathscr{Z}_{c+p,q-c} = -4x_{c+p}\overline{x_{c-q}}\langle T_{p+q}, T_0\rangle = -w_p\overline{w_{-q}}\langle T_{p+q}, T_0\rangle,$$

Second, suppose $m = p - c < 0$ and $n = c + q > 0$. Then, from Proposition 2 and Eq. (17) it follows that:

$$\mathscr{Z}_{p-c,c+q} = -4\overline{x_{c-p}}x_{c+q}\langle T_{p+q}, T_0\rangle = -\overline{w_{-p}}w_q\langle T_{p+q}, T_0\rangle,$$

Then, for $p < c$ and $q < c$:

$$\mathscr{W}_{p,q} = -\langle T_{p+q}, T_0\rangle\left(w_p\overline{w_{-q}} + \overline{w_{-p}}w_q\right) = \mathscr{Z}_{p+c,q-c} + \mathscr{Z}_{q+c,p-c}.$$

(4) The result follows immediately from Definition 1 and Eq. (17). □

Proof of Proposition 4

Write $Z(t) = e^{2\pi cti}V(t)$.

(1) Horizontal, vertical and diagonal lines in URP_X. Horizontal lines $(u, v) = (t, t_0)$ and vertical lines $(u, v) = (t_0, t)$:

$$\begin{aligned}\mathrm{URP}_X(u,v)^2 &= \|X(t)-X(t_0)\|^2\\ &= \left(\|X(t_0)\|^2+\frac{1}{2}\|V(t)\|^2\right)\\ &\quad -2Re\left(e^{2\pi cti}\langle V(t),X(t_0)\rangle\right)\\ &\quad +\frac{1}{2}Re\left(e^{4\pi cti}\langle V(t),\overline{V(t)}\rangle\right).\end{aligned}$$

The first, second and third term have frequencies in the ranges $\{0,\ldots,2d\}$, $\{c-d,\ldots,c+d\}$ and $\{2c-2d,\ldots,2c+2d\}$, respectively. Diagonal lines $(u,v)=(t+\tau_0,t)$:

$$\begin{aligned}\mathrm{URP}_X(u,v)^2 &= \|X(t+\tau_0)-X(t)\|^2\\ &= \frac{1}{2}\left\|e^{2\pi c\tau_0 i}V(t+\tau_0)-V(t)\right\|^2\\ &\quad +\frac{1}{2}Re\left(e^{4\pi cti}\langle e^{2\pi c\tau_0 i}V(t+\tau_0)-V(t),e^{-2\pi c\tau_0 i}\overline{V(t+\tau_0)}-\overline{V(t)}\rangle\right).\end{aligned}$$

The first and second term have frequencies in the ranges $\{0,\ldots,2d\}$ and $\{2c-2d,\ldots,2c+2d\}$, respectively.

(2) Horizontal, vertical and diagonal lines in URP_Z. Horizontal lines $(u,v)=(t,t_0)$ and vertical lines $(u,v)=(t_0,t)$:

$$\begin{aligned}\mathrm{URP}_Z(u,v)^2 &= \|Z(t)-Z(t_0)\|^2\\ &= \left(\|Z(t_0)\|^2+\|V(t)\|^2\right)\\ &\quad -2Re\left(e^{2\pi cti}\langle V(t),Z(t_0)\rangle\right).\end{aligned}$$

The first and second term have frequencies in the ranges $\{0,\ldots,2d\}$ and $\{c-d,\ldots,c+d\}$, respectively.
Diagonal lines $(u,v)=(t+\tau_0,t)$:

$$\mathrm{URP}_Z(u,v)^2=\|Z(t+\tau_0)-Z(t)\|^2=\left\|e^{2\pi c\tau_0 i}V(t+\tau_0)-V(t)\right\|^2.$$

The latter term has frequencies in the range $\{0,\ldots,2d\}$.

(3) The maximum of the first frequency range is lower than the minimum of the second frequency range if and only if $c>3d$. Similarly, the maximum of the second frequency range is lower than the minimum of the third frequency range if and only if $c>3d$.

References

1. Sipers, A., Borm, P., Peeters, R.: On the unique reconstruction of a signal from its unthresholded recurrence plot. Phys. Lett. A **375**(24), 2309–2321 (2011)
2. Eckmann, J.P., Oliffson Kamphorst, S., Ruelle, D.: Recurrence plots of dynamical systems. Europhys. Lett. **4**(9), 973–977 (1987)
3. Marwan, N., Romano, M.C., Thiel, M., Kurths, J.: Recurrence plots for the analysis of complex systems. Phys. Rep. **438**(5), 237–329 (2007)
4. Webber, C.L., Zbilut, J.P.: Dynamical assessment of physiological systems and states using recurrence plot strategies. J. Appl. Physiol. **76**(2), 965–973 (1994)
5. Website on recurrence plots and cross recurrence plots (2013). http://www.recurrence-plot.tk. Accessed 1 Nov 2013
6. Marwan, N.: How to avoid potential pitfalls in recurrence plot based data analysis. Int. J. Bifurcat. Chaos **21**(04), 1003–1017 (2011)
7. Takens, F.: Detecting strange attractors in turbulence. In: Rand, D., Young, L. (eds.) Dynamical Systems and Turbulence. Lecture Notes in Mathematics, pp. 366–381. Springer, Berlin (1981)
8. Chen, Y., Yang, H.: Multiscale recurrence analysis of long-term nonlinear and nonstationary time series. Chaos, Solitons Fractals **45**(7), 978–987 (2012)
9. McGuire, G., Azar, N.B., Shelhamer, M.: Recurrence matrices and the preservation of dynamical properties. Phys. Lett. A **237**(1), 43–47 (1997)
10. Hirata, Y., Horai, S., Aihara, K.: Reproduction of distance matrices and original time series from recurrence plots and their applications. European Phys. J., Special Topics **164**(1), 13–22 (2008)
11. Jie, L., Shu-Ting, S., Jun-Chan, Z.: Comparison study of typical algorithms for reconstructing time series from the recurrence plot of dynamical systems. Chin. Phys. B **22**(1), 010–505 (2013)
12. Robinson, G., Thiel, M.: Recurrences determine the dynamics. Chaos **19**(2), 023–104 (2009)
13. Thiel, M., Romano, M.C., Kurths, J.: How much information is contained in a recurrence plot? Phys. Lett. A **330**(5), 343–349 (2004)
14. Romano, M.C., Thiel, M., Kurths, J., von Bloh, W.: Multivariate recurrence plots. Phys. Lett. A **330**(3–4), 214–223 (2004)
15. Krauss, G.L., Fisher, R.S.: The Johns Hopkins Atlas of Digital EEG, chap. 2, pp. 58–61. Johns Hopkins University Press, Baltimore (2006)
16. Bajaj, V., Pachori, R.: Classification of seizure and nonseizure EEG signals using empirical mode decomposition. Inf. Technol. Biomed. IEEE Trans. **16**(6), 1135–1142 (2012)
17. Bajaj, V., Pachori, R.: EEG signal classification using empirical mode decomposition and support vector machine. In: Proceedings of the International Conference on Soft Computing for Problem Solving (SocProS 2011), vol. 131, pp. 623–635. Springer, India (2012), 20–22 Dec 2011
18. Etévenon, P., Lebrun, N., Clochon, P., Perchey, G., Eustache, F., Baron, J.C.: High temporal resolution dynamic mapping of instantaneous EEG amplitude modulation after tone-burst auditory stimulation. Brain Topogr. **12**(2), 129–137 (1999)
19. Falk, T.H., Fraga, F.J., Trambaiolli, L., Anghinah, R.: EEG amplitude modulation analysis for semi-automated diagnosis of Alzheimer's disease. EURASIP J Adv. Signal Process. **2012**(1), 192 (2012)
20. Pachori, R.B., Bajaj, V.: Analysis of normal and epileptic seizure EEG signals using empirical mode decomposition. Comput. Methods Programs Biomed. **104**(3), 373–381 (2011)